Applied Catalysis B: Environmental 306 (2022) 121131

Contents lists available at ScienceDirect

Applied Catalysis B: Environmental

journal homepage: www.elsevier.com/locate/apcatb

Understanding the self-catalyzed decomplexation mechanism of Cu-EDTA in $Ti_3C_2T_x$ MXene/peroxymonosulfate process

Daoyuan Zu [a], Haoran Song [b], Changping Li [b,*], Yuwei Wang [b], Rong Du [c,d], Rui Zhou [b], Wei Zhang [e], Shiting Pan [b], Yang Cai [b], Yongming Shen [a], Zhifeng Yang [a,*]

[a] Guangdong Provincial Key Laboratory of Water Quality Improvement and Ecological Restoration for Watersheds, Institute of Environmental & Ecological Engineering, Guangdong University of Technology, Guangzhou, Guangdong 510006, China
[b] Research Center for Eco-environmental Engineering, Dongguan University of Technology, Dongguan, Guangdong 523808, China
[c] Institute of High Energy Physics Chinese Academy of Sciences, Beijing 100049, China
[d] Spallat Neutron Source Science Centre, Dongguan, Guangdong 523808, China
[e] School of Environmental and Material Engineering, Yantai University, Yantai, Shandong 264005, China

ARTICLE INFO

Keywords:
Self-catalyzed decomplexation
Cu-EDTA
$Ti_3C_2T_x$ MXene
Peroxymonosulfate
Cu(II)/Cu(I) cycle

ABSTRACT

Self-catalyzed decomplexation of Cu-ethylene diamine tetraacetic acid complex (Cu-EDTA) and recovery of Cu without addition of extraneous transition metals were achieved in $Ti_3C_2T_x$ MXene/peroxymonosulfate ($Ti_3C_2T_x$/PMS) process. Free radical quenching experiments and electron spin resonance (ESR) measurements demonstrated that both hydroxyl radical ($HO^•$) and sulfate radical ($SO_4^{•-}$) contributed to the degradation of Cu-EDTA. Activation of PMS by $Ti_3C_2T_x$ initiated Cu-EDTA decomplexation and released free Cu ions. Then, the formation of Ti-O-Cu bonds between Cu ions and $Ti_3C_2T_x$ accelerated the electron transfer from $Ti_3C_2T_x$ to Cu(II) and triggered Cu(II)/Cu(I) cycle, which further enhanced PMS activation and led to the self-catalyzed decomplexation of Cu-EDTA. Simultaneous recovery of Cu was achieved due to the excellent absorption performance of negative charged $Ti_3C_2T_x$ towards Cu ions. This study revealed the self-catalyzed decomplexation mechanism of Cu-EDTA in the $Ti_3C_2T_x$/PMS process and provided a feasible strategy for heavy metal complexes treatment.

1. Introduction

Wastewater discharged from electroplating, printed circuit board and mining industries always contains multiple chelating agents and heavy metals, which leads to the formation of heavy metal complexes [1,2]. It was reported that heavy metal complexes possessed potential harmfulness towards animals, plants and humans [3,4]. The characters of heavy metal complexes, such as strong migration, poor affinity with various adsorbents and high stability under wide pH range, make those difficult to be removed by conventional wastewater treatment technologies including adsorption, alkaline precipitation and ion exchange [5,6]. Therefore, it is urgent to develop efficient technologies to remove heavy metal complexes from wastewater. A two-steps process, oxidative decomplexation combined with precipitation, has been proved to be an efficient strategy for removing heavy metal complexes [7]. Heavy metal complexes were firstly oxidized by various oxidants, then the released heavy metals were removed by precipitation. Advanced oxidation processes (AOPs) including Fenton [8], electro-Fenton [9], UV/H_2O_2 [10], photocatalysis [11] and ozonation [12] have been confirmed to be effective in the decomplexation of heavy metal complexes due to the generation of reactive oxygen species. However, the two-steps process (AOPs combined with precipitation) for removing heavy metal complexes was still complicated and costly, which consumed extraneous chemicals and energy.

In Fenton and Fenton-like oxidation processes, low-valent transition metal ions or oxides were always employed to activate hydrogen peroxide (H_2O_2) and peroxymonosulfate (PMS). Unfortunately, Fenton and Fenton-like processes with transition metal ions possessed natural defects in removing heavy metal complexes because that the extraneous transition metals would form the new complexes with chelating agents and caused secondary pollution such as metal leakage, sludge production and chromaticity rise [13]. It is well known that heavy metal complexes inherently contain various transition metals, such as Fe, Cu and Co. If these transition metal ions inherent in heavy metal complexes could be utilized to activate H_2O_2 or PMS, removal of heavy metal complexes will consume no extraneous transition metal ions.

* Corresponding authors.
E-mail addresses: licpbit@hotmail.com (C. Li), zfyang@gdut.edu.cn (Z. Yang).

https://doi.org/10.1016/j.apcatb.2022.121131
Received 18 October 2021; Received in revised form 12 January 2022; Accepted 20 January 2022
Available online 22 January 2022

Our previous work indicated that $Ti_3C_2T_x$ MXene could significantly enhance PMS activation by triggering Fe^{3+}/Fe^{2+} cycle with ultra-low metal consumption at the μg L^{-1} level [14]. MXene could also reduce other high-valent metals, such as Cu (II) [15], Cr (Vl) [16], Ag (I) [17], U (VI) [18] and Re (VII) [19], to their corresponding low-valent states. Additionally, $Ti_3C_2T_x$ MXene exhibited outstanding absorption performance towards Cu [15], Cr [16], Pb [20] and Hg [21], due to its large specific surface area, abundant surface functional groups (-F, -O and -OH denoted as T_x) and surface electronegativity. Therefore, application of $Ti_3C_2T_x$ MXene in Fenton-like process may realize the efficient decomplexation of heavy metal complexes and recovery of heavy metals without addition of extraneous transition metals and precipitants.

Cu-ethylene diamine tetraacetic acid complex (Cu-EDTA), a module of heavy metal complexes, was used as the target pollutant in this work. The performance of Cu-EDTA decomplexation and Cu recovery was firstly investigated in $Ti_3C_2T_x$/PMS process. Then, the primary reactive species were identified by free radical quenching experiments and electron spin resonance (ESR) measurements. The intermediate species dominating PMS activation and the role of $Ti_3C_2T_x$ MXene were investigated, respectively. Meanwhile, the evolution of Cu inherent in Cu-EDTA was explored in detail. Influences of $Ti_3C_2T_x$ concentration, PMS concentration and solution pH were also evaluated. The recycling stability of $Ti_3C_2T_x$ and treatment of realistic effluent containing Cu-EDTA were investigated to evaluate the potential application of $Ti_3C_2T_x$/PMS process. At last, a novel self-catalyzed decomplexation mechanism of Cu-EDTA was proposed. This work provided a feasible strategy for the efficient decomplexation of Cu-EDTA and recovery of Cu without addition of extraneous transition metals and precipitants.

2. Experimental section

2.1. Materials and chemicals

Cu-ethylene diamine tetraacetic acid complex (Cu-EDTA), peroxymonosulfate (PMS, $KHSO_5{\cdot}0.5\ KHSO_4{\cdot}0.5\ K_2SO_4$), copper sulfate ($CuSO_4$), cupric oxide (CuO), cuprous oxide (Cu_2O), sulfamethoxazole (SMX), sodium iminodiacetate dibasic hydrate (IMDA) and N-(2-aminoethyl) glycine (EDMA) were purchased from Aladdin (Shanghai, China). N-(carboxymethyl)-N-2-(carboxymethyl) aminoethyl-trisodium salt (ED3A) was obtained from Macklin (Shanghai, China). 5,5-dimthyl-1-pyrrolidine N-oxide (DMPO) and ethylenediamine-N, N′-diacetic acid (ED2A) were provided by Sigma-Aldrich (MO, USA). Methanol of HPLC grade from TEDIA Co., Ltd. (USA) and Ti_3AlC_2 ceramic powder (500 mesh) from Kaikai Ceramics Co., Ltd (Yantai, China) were employed for this study. All solutions were prepared using ultrapure water.

2.2. Preparation of $Ti_3C_2T_x$ MXene

$Ti_3C_2T_x$ MXene was prepared by etching Ti_3AlC_2 powders [22]. Typically, 5 g of Ti_3AlC_2 powder was added into 100 ml HCl/LiF solution. The suspension solution was placed in 40 °C water bath for 48 h. Then, the mixture was repeatedly washed with ultrapure water. The $Ti_3C_2T_x$ MXene slurry was diluted with ultrapure water and shocked for 12 h. After that, the mixture was centrifuged at 3000 rpm for 30 min. The centrifuge supernatant solution was collected and vacuum freeze-dried at − 20 °C for 48 h.

2.3. Experimental procedure

All degradation experiments were performed in a 100 ml quartz beaker. Solution pH was adjusted by NaOH solution (0.01 M) and H_2SO_4 solution (0.01 M). The desired amount of Cu-EDTA, $Ti_3C_2T_x$ and PMS were added into 100 ml ultrapure water. At predetermined time intervals, 1 ml of the solution was collected with a pipette and filtered through a 0.22 μm poly-tetra-fluoroethylene (PTFE) membrane into vials containing excess methanol.

2.4. Characterization and analysis methods

The concentrations of Cu-EDTA and SMX were measured on a high-performance liquid chromatography (HPLC, Agilent 1260 Infinity, USA) instrument. The Agilent C18 chromatographic column (4.6 mm × 250 mm×5 μm) was used to separate chemicals. The elution for Cu-EDTA was consisted of methanol and acetic acid (17.5 mM) at the 2:98 (v/v) ratio. The mobile phase for SMX separation was methanol and ultrapure water with a 60:40 ratio. The flow rate was 1 ml min^{-1}. The detection wavelength was set at 254 nm for Cu-EDTA and 260 nm for SMX. The concentration of total copper was measured using the inductively coupled plasma mass spectrometry (ICP-MS, Thermo Scientific, USA). PMS concentration was determined by the spectrophotometric method [23]. The intermediate products of Cu-EDTA were identified using an ultra-performance liquid chromatography-mass spectrometry (UPLC-MS, Q Exactive Focus Thermo Fisher, USA). Electron spin resonance (ESR) measurements were performed on a Bruker A200 spectrometer. The surface elementary composition of fresh and used $Ti_3C_2T_x$ was analyzed using an X-ray photoelectron spectroscopy (XPS, ESCALAB250, USA). The X-ray diffraction (XRD) patterns were obtained using a Bruker D8 Advance diffractometer. X-ray adsorption spectroscopy was carried out on the Beijing Synchrotron Irradiation Facility (BSRF, 1W1B).

3. Results and discussion

3.1. Cu-EDTA removal and Cu recovery in $Ti_3C_2T_x$/PMS process

The performance of $Ti_3C_2T_x$/PMS process for the Cu-EDTA removal and Cu recovery without addition of extraneous transition metals and precipitants was investigated. As shown in Fig. 1a, Cu-EDTA removal efficiency was less than 5% in PMS alone process within 20 min reaction time. Addition of $Ti_3C_2T_x$ in Cu-EDTA solution in the absence of PMS increased the removal efficiency of Cu-EDTA to about 8%, which could be attributed to the adsorption of Cu-EDTA on $Ti_3C_2T_x$. As expected, $Ti_3C_2T_x$/PMS process achieved 100% removal efficiency of Cu-EDTA within 3 min reaction time, significantly higher than those of PMS alone process and $Ti_3C_2T_x$ process. Recovery of Cu is always needed in Cu-EDTA treatment process. As shown in Fig. 1b, the recovery efficiency of Cu in $Ti_3C_2T_x$/PMS process was about 84% after 20 min reaction time, remarkably higher than those in PMS process (about 4%) and $Ti_3C_2T_x$ process (about 7%). The above results suggested that the efficient removal of Cu-EDTA and recovery of Cu were achieved in $Ti_3C_2T_x$/PMS process.

3.2. Identification of primary reactive species

Hydroxyl radical ($HO^{\bullet}$) and sulfate radical ($SO_4^{\bullet-}$) were always generated from PMS activation [24–26]. In order to explore the contribution of $HO^{\bullet}$ or $SO_4^{\bullet-}$, methanol was used as the quenching agent for $HO^{\bullet}$ and $SO_4^{\bullet-}$, while tert-butanol (TBA) was used as the quenching agent for $HO^{\bullet}$ [27–29]. As shown in Fig. 2a, Cu-EDTA removal was completely inhibited in the presence of 200 mM methanol, which indicated that $HO^{\bullet}$ or $SO_4^{\bullet-}$ was generated in oxidation process. Addition of tert-butanol (200 mM) also inhibited the removal of Cu-EDTA in $Ti_3C_2T_x$/PMS process, but the inhibitory effect was slightly less than that in the presence of methanol. Hence, both $HO^{\bullet}$ and $SO_4^{\bullet-}$ contributed to the removal of Cu-EDTA.

Furthermore, ESR measurements were performed to identify the generation of $HO^{\bullet}$ and $SO_4^{\bullet-}$. As shown in Fig. 2b, no obvious peak was observed in the spectrum of PMS/Cu-EDTA process, while DMPO-$HO^{\bullet}$ adduct and DMPO-$SO_4^{\bullet-}$ adduct signals were observed in the spectrum of $Ti_3C_2T_x$/PMS process (Fig. 2c), which verified that $Ti_3C_2T_x$ could activate PMS [30]. The signal intensity of DMPO-$HO^{\bullet}$ adduct and

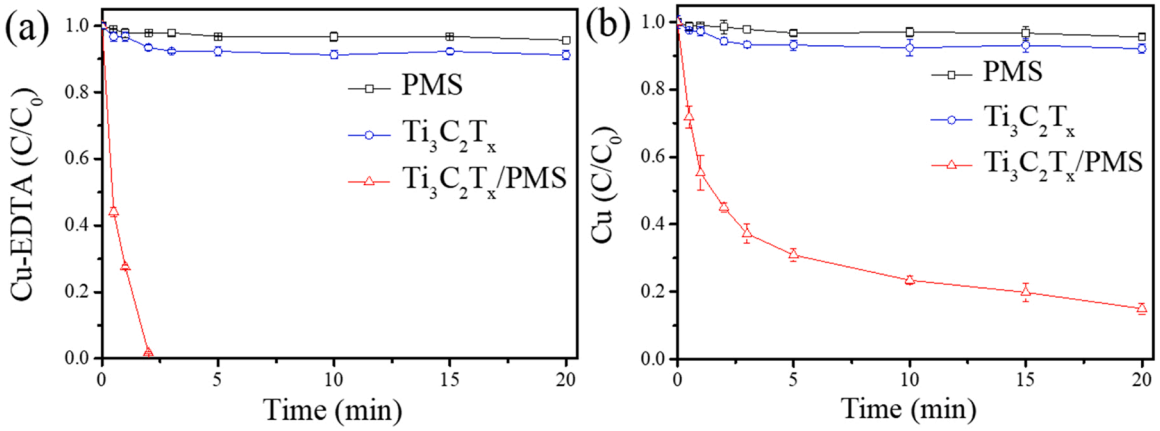

Fig. 1. Removal of Cu-EDTA (a) and recovery of Cu (b) in $Ti_3C_2T_x$/PMS process. Conditions: $[PMS]_0 = 0.2$ mM, $[Cu\text{-}EDTA]_0 = 10$ μM, $[Ti_3C_2T_x]_0 = 60$ mg L^{-1}, $[pH]_0 = 4.0$, and T = 25 °C.

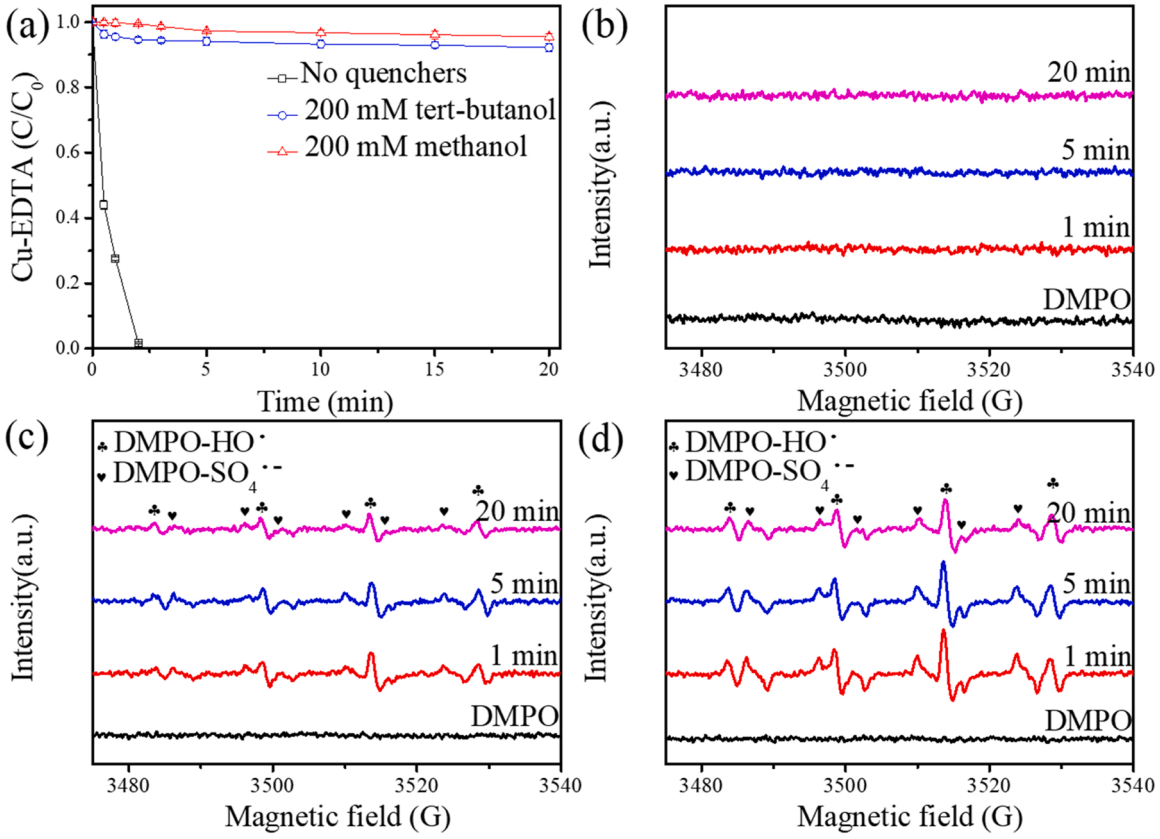

Fig. 2. (a) Effect of methanol and tert-butanol on Cu-EDTA removal in $Ti_3C_2T_x$/PMS process. ESR spectrum of (b) Cu-EDTA/PMS, (c) $Ti_3C_2T_x$/PMS, (d) $Ti_3C_2T_x$/PMS/Cu-EDTA. Conditions: $[DMPO]_0 = 40$ mM, $[PMS]_0 = 0.2$ mM, $[Cu\text{-}EDTA]_0 = 10$ μM, $[Ti_3C_2T_x]_0 = 60$ mg L^{-1}, $[pH]_0 = 4.0$, and T = 25 °C.

DMPO-$SO_4^{\bullet-}$ adduct was increased after addition of Cu-EDTA into $Ti_3C_2T_x$/PMS process (Fig. 2d), suggesting that Cu-EDTA promoted the generation of $HO^{\bullet}$ and $SO_4^{\bullet-}$ in $Ti_3C_2T_x$/PMS process. The generation of $HO^{\bullet}$ and $SO_4^{\bullet-}$ was related to the consumption of PMS. To further evaluate the promotion of $Ti_3C_2T_x$ by Cu-EDTA for PMS activation, PMS decomposition in various processes was measured with the spectrophotometric method (Figs. S1-S2) [23]. The negligible decomposition of PMS occurred in Cu-EDTA solution, suggesting that Cu-EDTA could not activate PMS (Fig. S2). A slight decomposition of PMS (about 7% decomposition efficiency) occurred in $Ti_3C_2T_x$/PMS process, while the rapid decomposition of PMS (about 67% decomposition efficiency) was observed after addition of Cu-EDTA into $Ti_3C_2T_x$/PMS process. The above results implied that Cu-EDTA could significantly enhance PMS decomposition to generate more $HO^{\bullet}$ and $SO_4^{\bullet-}$ in the presence of $Ti_3C_2T_x$.

3.3. The involvement of Cu(I)

Addition of Cu-EDTA into $Ti_3C_2T_x$/PMS process could obviously promote the generation of $HO^{\bullet}$ and $SO_4^{\bullet-}$. However, the underlying mechanism was still unclear. It was reported that some decomposition products of Cu-EDTA could activate persulfate [10,31]. Therefore, the decomposition products of Cu-EDTA in $Ti_3C_2T_x$/PMS process were identified with mass spectrometry. Mass spectrometry analysis

demonstrated that the decomposition products of Cu-EDTA mainly included N-(carboxymethyl)-N-2-(carboxymethyl) aminoethyl trisodium salt (ED3A), ethylenediamine-N, N '-diacetic acid (ED2A), sodium iminodiacetate dibasic hydrate (IMDA), N-(2-aminoethyl) glycine (EDMA) (Fig. S3). Then, activation of PMS by Cu-EDTA, Cu-ED3A, Cu-ED2A, Cu-IMDA and Cu-EDMA was investigated sulfamethoxazole (SMX) as the model pollutant, respectively. As shown in Fig. 3a, Cu-EDTA/PMS, Cu-ED3A/PMS, Cu-ED2A/PMS, Cu-IMDA/PMS and Cu-EDMA/PMS processes all induced negligible removal of SMX. Interestingly, addition of $Ti_3C_2T_x$ into the above processes all remarkably promoted SMX removal (Fig. 3b). The above results indicated that the decomposition products of Cu-EDTA could not activate PMS in the absence of $Ti_3C_2T_x$ MXene. There must exist some undiscovered reactions related to $Ti_3C_2T_x$ and copper-containing complexes which contributed to PMS activation.

In addition to the decomplexation products of Cu-EDTA, Cu ions were also released in oxidation process. Our previous work indicated that $Ti_3C_2T_x$ could reduce Fe^{3+} to Fe^{2+}, which significantly enhanced PMS activation [14]. Therefore, low-valent Cu species might be generated in $Ti_3C_2T_x$/PMS/Cu-EDTA process. Additionally, reduction of Cu^{2+} by $Ti_3C_2T_x$ also generated copper oxides including CuO and Cu_2O [15]. It is well known that copper oxides could activate PMS [32–34]. Therefore, SMX removal experiments in Cu^{2+}/PMS, $Ti_3C_2T_x$/PMS, CuO/PMS, Cu_2O/PMS and $Ti_3C_2T_x/Cu^{2+}$/PMS process were conducted to investigate the contribution of different copper-containing species to PMS activation. Fig. 3c showed that the removal efficiency of SMX in Cu^{2+}/PMS, CuO/PMS and Cu_2O/PMS process was negligible (less than 4%) within 20 min reaction time. Partial removal of SMX (about 11%) in $Ti_3C_2T_x$/PMS process could be attributed to PMS activation by the low-valent Ti of $Ti_3C_2T_x$ [30]. It was worth noting that addition of Cu^{2+} into $Ti_3C_2T_x$/PMS process generated remarkably higher removal efficiency of SMX (100% removal efficiency within 8 min reaction time) than those in Cu^{2+}/PMS, CuO/PMS and Cu_2O/PMS processes. Therefore, the contribution of Cu_2O, CuO and Cu^{2+} to PMS activation was insignificant and the reaction between Cu^{2+} and $Ti_3C_2T_x$ played the key role in PMS activation.

Based on the above results, it is reasonable to speculate that addition of $Ti_3C_2T_x$ into Cu^{2+}/PMS process might trigger the Cu(II)/Cu(I) cycle and the generated Cu(I) dominated PMS activation. In order to verify this hypothesis, detection of Cu(I) using neocuproine (NCP) as the chromogenic agent was performed [27]. As shown in Fig. 3d, an obvious absorption peak at 459 nm corresponding to Cu(I)-NCP complex could be observed when $Ti_3C_2T_x$ was added into the mixed solution Cu^{2+} and NCP, indicating that $Ti_3C_2T_x$ could reduce Cu(II) to Cu(I).

In order to furtherly explore the evolution of Cu^{2+}, XPS analysis was performed. As shown in Fig. 4b, two obvious Cu 2p peaks at 932.7 eV and 952.7 eV corresponding to Cu(I) and Cu(II) were observed in the used $Ti_3C_2T_x$ sample [15]. The formation of Cu(I) in the used $Ti_3C_2T_x$ sample indicated that Cu(II) was indeed reduced to Cu(I). In addition, the peak intensity of the Ti-O bond at 459 eV was significantly increased after reaction (Fig. 4c-d), which also proved that Cu^{2+} oxidized $Ti_3C_2T_x$. X-ray diffractometer (XRD) characterization also indicated that oxidation of $Ti_3C_2T_x$ occurred in $Ti_3C_2T_x$/PMS/Cu-EDTA process. Only one obvious diffraction peak at 6.2° corresponding to the (002) plane of $Ti_3C_2T_x$ was observed in the fresh $Ti_3C_2T_x$ sample (Fig. S4). After reaction, a new peak located at 25.4° was generated, which belonged to the (101) plane of anatase TiO_2. Fig. 4e-f provided the O 1s XPS analysis of fresh and used $Ti_3C_2T_x$. The peaks of fresh $Ti_3C_2T_x$ located at 529.6 eV, 531.7 eV and 533 eV were attributed to the Ti-O bond, C-Ti-O bond and Ti-OH bond [35], respectively. A new peak at 530.5 eV appeared after reaction, which was assigned to Cu-O bond indicating the Cu adsorption on $Ti_3C_2T_x$.

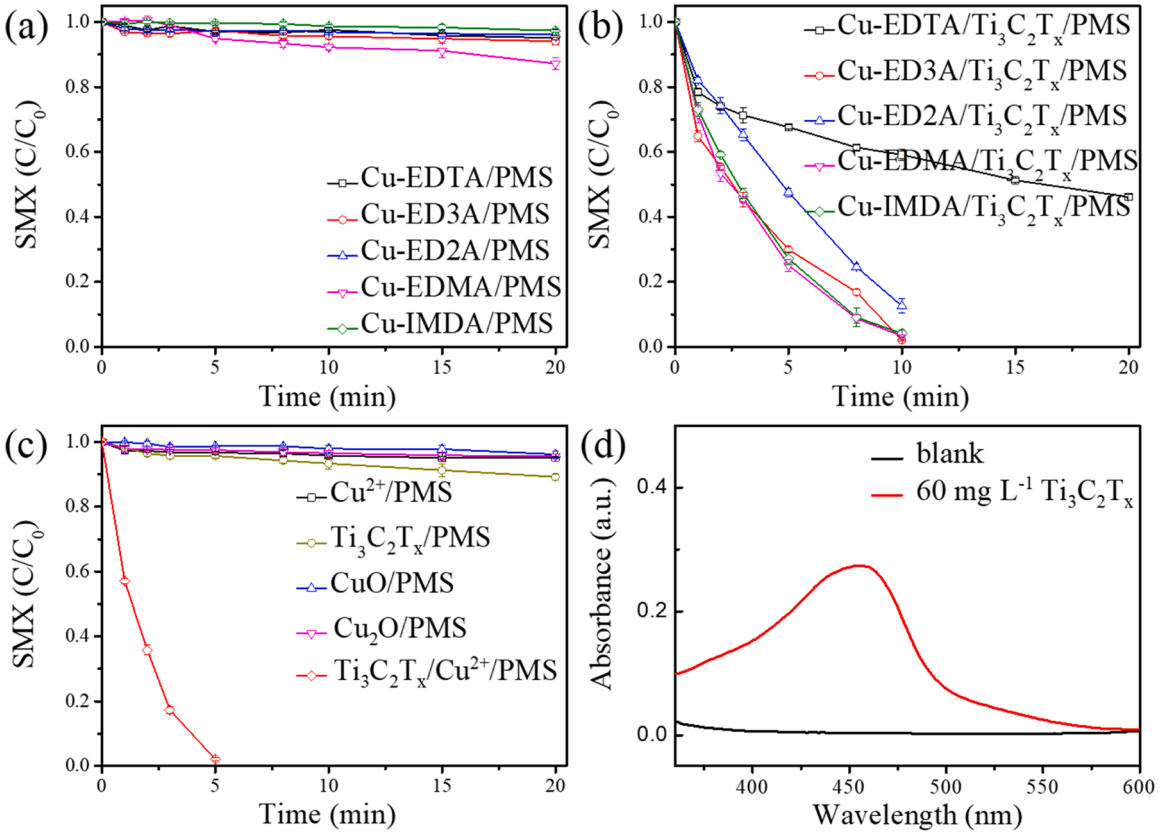

Fig. 3. Activation of PMS by the decomplexation products of Cu-EDTA (a-b) in the absence or presence of $Ti_3C_2T_x$ MXene and (c) copper-containing species. Conditions: $[\text{Decomplexation products}]_0 = 10\ \mu M$, $[\text{copper-containing species}]_0 = 10\ \mu M$, $[SMX]_0 = 5\ \mu M$, $[PMS]_0 = 0.2\ mM$, $[pH]_0 = 4.0$, and $T = 25\ ^\circ C$. (d) Ultraviolet-visible spectrum of $Ti_3C_2T_x/Cu^{2+}$ in the presence of neocuproine. Conditions: $[Cu^{2+}]_0 = 5\ mM$, $[\text{neocuproine}]_0 = 0.4\ mM$, $T = 25\ ^\circ C$, and pH= 4.0.

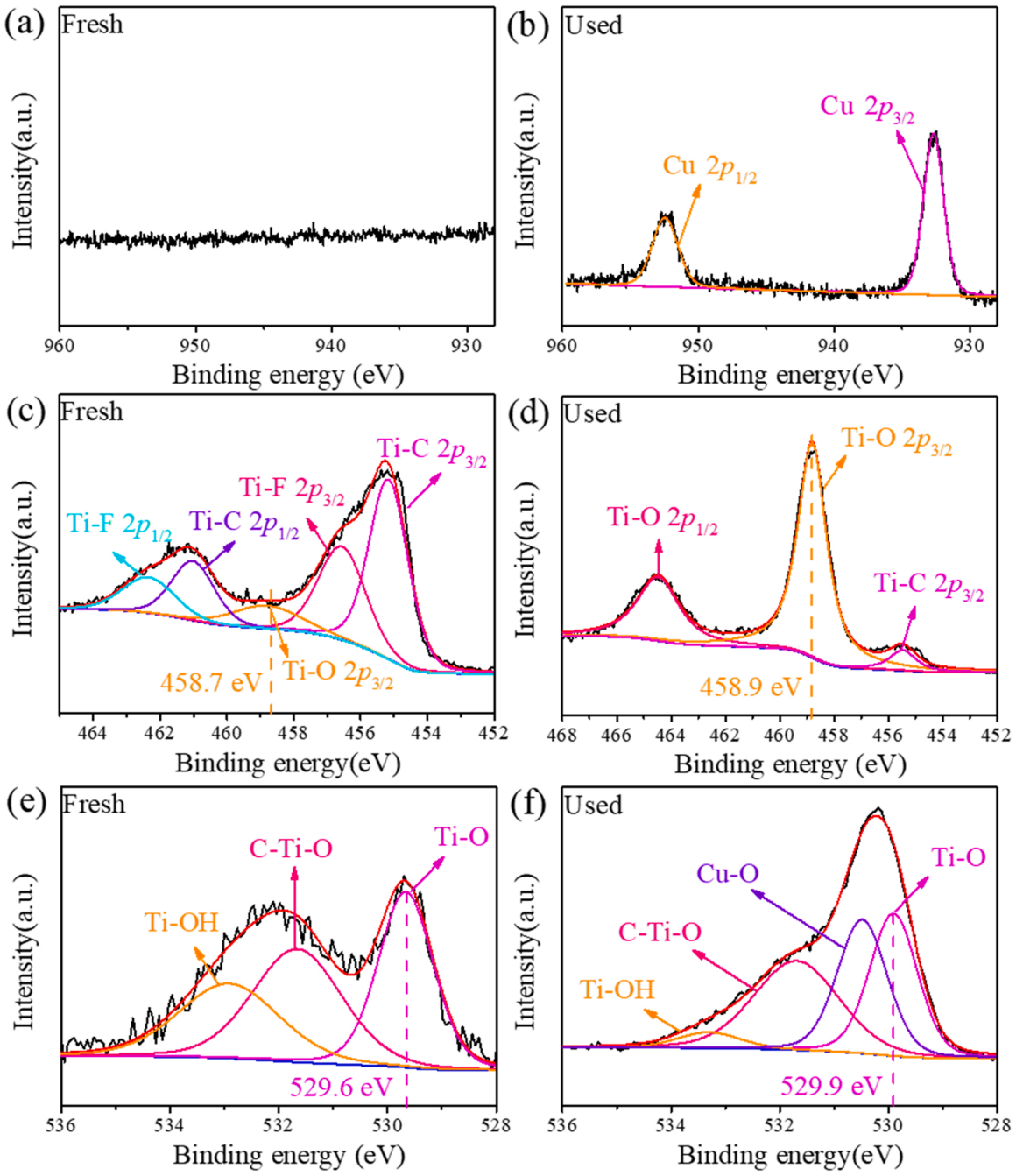

Fig. 4. The Cu 2p (a and b), Ti 2p (c and d) and O 1 s (e and f) XPS spectrum of fresh and used $Ti_3C_2T_x$. Conditions: $[Ti_3C_2T_x]_0 = 60$ mg L^{-1}, $[Cu^{2+}]_0 = 5$ mM, T = 25 °C, and pH= 4.0.

3.4. Enhanced electron transfer by the formation of Ti-O-Cu bond

Because of the strong electronegativity of $Ti_3C_2T_x$, the released Cu ions in decomplexation process would be adsorbed on the surface of $Ti_3C_2T_x$. The surface of $Ti_3C_2T_x$ contains abundant functional groups (-F, -O and –OH denoted as T_x). The observation of Cu-O bond (i.e. Ti-O-Cu bond) in Fig. 4f suggested that there existed strong interaction between Cu ions and $Ti_3C_2T_x$ MXene. In order to investigate the electronic and local coordination of Cu ions in $Ti_3C_2T_x$, X-ray absorption near-edge spectroscopy (XANES) and extended X-ray absorption fine structure (EXAFS) analyses were conducted. As shown in Fig. 5a, the white line position of $Ti_3C_2T_x$-Cu sample located between those of CuO and Cu_2O, suggesting that the valance state of Cu in $Ti_3C_2T_x$-Cu was between + 1 and + 2. Fig. 5b provided the k^3-weighted EXAFS Fourier transform spectra in R space. The peak at about 1.47 Å corresponding to the Cu-O bond of CuO and Cu_2O was also observed in $Ti_3C_2T_x$-Cu sample. This result indicated that Cu ions were bonded with oxygen-containing functional groups on the surface of $Ti_3C_2T_x$ and formed Ti-O-Cu bond. XPS analysis provided another evidence for the formation of Ti-O-Cu bond. The peaks assigned to Ti-O bond in Ti 2p (458.7–458.9 eV) and the O 1s (529.6–529.9 eV) XPS spectrum were both shifted to higher energy values (Fig. 4e-f), indicating the formation of the Ti-O-Cu bond [15,36].

Compared with homogeneous reaction, the formation of Ti-O-Cu bond could shorten the electron transfer distances from $Ti_3C_2T_x$ to Cu (II), which could accelerate Cu(II)/Cu(I) cycle and enhance PMS activation. Ascorbic acid (AA) and hydroxylamine (HA) were usually used to trigger M^{n+1}/M^{n+} cycle in Fenton-like process [37,38]. In order to

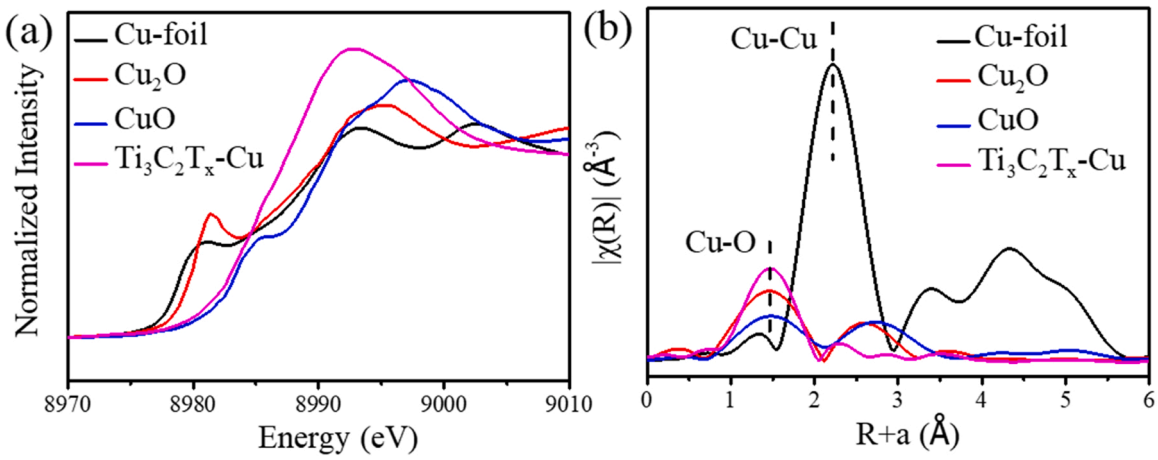

Fig. 5. (a) Normalized Cu K-edge XANES spectra and (b) k^3-weighted EXAFS Fourier transform spectra of Cu-foil, Cu_2O, CuO and $Ti_3C_2T_x$-Cu.

verify the superiority of Ti-O-Cu bond, the comparation between $Ti_3C_2T_x$ with AA/HA for SMX removal was performed (Fig. 6). The removal efficiency of SMX in AA/Cu^{2+}/PMS and HA/Cu^{2+}/PMS processes was 4.1% and 43.5% within 20 min reaction time, far lower than that in $Ti_3C_2T_x$/Cu^{2+}/PMS process (99% removal efficiency within 5 min reaction time). The quasi-first-order removal rate of SMX in $Ti_3C_2T_x$/Cu^{2+}/PMS process was 0.6971 min^{-1}, about 21.3 times and 257.2 times higher than those in HA/Cu^{2+}/PMS (0.0313 min^{-1}) and AA/Cu^{2+}/PMS (0.0027 min^{-1}) processes (Fig. S5).

3.5. Influences of $Ti_3C_2T_x$ concentration, PMS concentration and solution pH

Influences of $Ti_3C_2T_x$ concentration, PMS concentration and solution pH on Cu-EDTA removal and Cu recovery were investigated, respectively. As shown in Fig. 7a, increase of $Ti_3C_2T_x$ concentration from 20 mg L^{-1} to 100 mg L^{-1} significantly enhanced Cu-EDTA removal. Cu-EDTA could be completely removed within 20 min reaction time when addition of 20 mg L^{-1} $Ti_3C_2T_x$ and 2 min when the $Ti_3C_2T_x$ concentration was increased to 100 mg L^{-1}. The recovery efficiency of Cu was increased from 36.2% to 97.9% with increasing the initial concentration of $Ti_3C_2T_x$ from 20 mg L^{-1} to 100 mg L^{-1} (Fig. 7b). The recovery efficiency of Cu was much lower than the removal efficiency of Cu-EDTA under the identical reaction conditions. This phenomenon could be ascribed to the incomplete degradation of Cu-EDTA. The decomposition products of Cu-EDTA including ED3A, ED2A, IMDA and EDMA (Fig. S3) complexed with Cu ions, leading to that the recovery curves of Cu lagged behind the removal curves of Cu-EDTA.

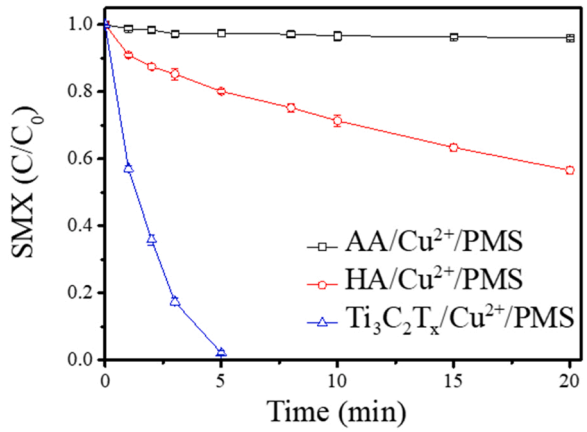

Fig. 6. Effect of various reducing agents on SMX removal in Cu^{2+}/PMS process. Conditions: $[reducing\ agent]_0 = 0.36$ mM, $[PMS]_0 = 0.2$ mM, $[SMX]_0 = 5$ μM, $[pH]_0 = 4.0$, and T = 25 °C.

The removal efficiency of Cu-EDTA was increased with increasing PMS concentration from 0.1 mM to 1.0 mM (Fig. 7c). The consumed time for complete removal of Cu-EDTA decreased from about 6 min in the presence of 0.1 mM PMS to less than 1 min in the presence of 1 mM PMS. The recovery efficiency of Cu was firstly increased from 76% to 85% with increasing PMS concentration from 0.1 mM to 0.2 mM and then decreased to 76% and 64% with further increasing PMS concentration to 0.5 mM and 1.0 mM (Fig. 7d). Faster removal of Cu-EDTA at higher concentration of PMS suggested that more radicals were generated and attacked Cu-EDTA. The XPS analysis (Fig. 4) and XRD pattern (Fig. S4) had verified that the oxidation of $Ti_3C_2T_x$ occurred in $Ti_3C_2T_x$/PMS process. Therefore, the decrease of Cu recovery efficiency with increasing PMS concentration was possibly attributed to the deterioration of Cu adsorption on $Ti_3C_2T_x$ when excessive radicals oxidized $Ti_3C_2T_x$.

In order to verify the above inference, recovery of Cu was investigated in $Ti_3C_2T_x$/PMS process followed by alkaline precipitation. As shown in Fig. S6, the recovery efficiency of Cu was up to 89.8% in $Ti_3C_2T_x$/PMS/alkaline precipitation process when the PMS concentration was 1 mM, significantly higher than 64% in $Ti_3C_2T_x$/PMS process. When the PMS concentration was less than 0.2 mM, the recovery efficiency of Cu in $Ti_3C_2T_x$/PMS process was closed to that in $Ti_3C_2T_x$/PMS/alkaline precipitation process. Cu recovery depended on oxidative decomplexation and absorption. The incomplete decomplexation of Cu-EDTA at the low concentration of PMS and excessive oxidation of $Ti_3C_2T_x$ at the high concentration of PMS would deteriorate Cu recovery.

Solution pH always played an important role in the Fenton-like reaction and adsorption process [15,39]. As expected, increase of solution pH from 3.0 to 4.0 obviously promoted Cu-EDTA removal (Fig. 7e). Complete removal of Cu-EDTA was achieved within 3 min under pH of 4.0, remarkably less than that of 15 min under pH of 3.0. This phenomenon could be attributed to the negative effect of H^+ toward PMS activation [40]. PMS ($pK_{a1}<0$, $pK_{a2}=9.4$) [39] mainly existed as HSO_5^- form under the investigated pH range (3.0–7.0). H^+ added positive charge to HSO_5^-, which hindered the interaction of HSO_5^- with the positively charged metal ions [39,40]. A further rise of pH to 5.0 inhibited Cu-EDTA removal compared with that under pH of 4.0 and the inhibitory effect was strengthened with increasing pH to 6.0 and 7.0. This was because the released Cu ions began to precipitate under high pH conditions (Fig. S7-8).

Similarly, the recovery efficiency of Cu was increased with increasing pH from 3.0 to 4.0 and then decreased when further increase of solution pH to 5.0, 6.0 and 7.0 (Fig. 7f). Cu recovery depended on Cu-EDTA decomplexation and Cu ions adsorption. The Zeta potential of

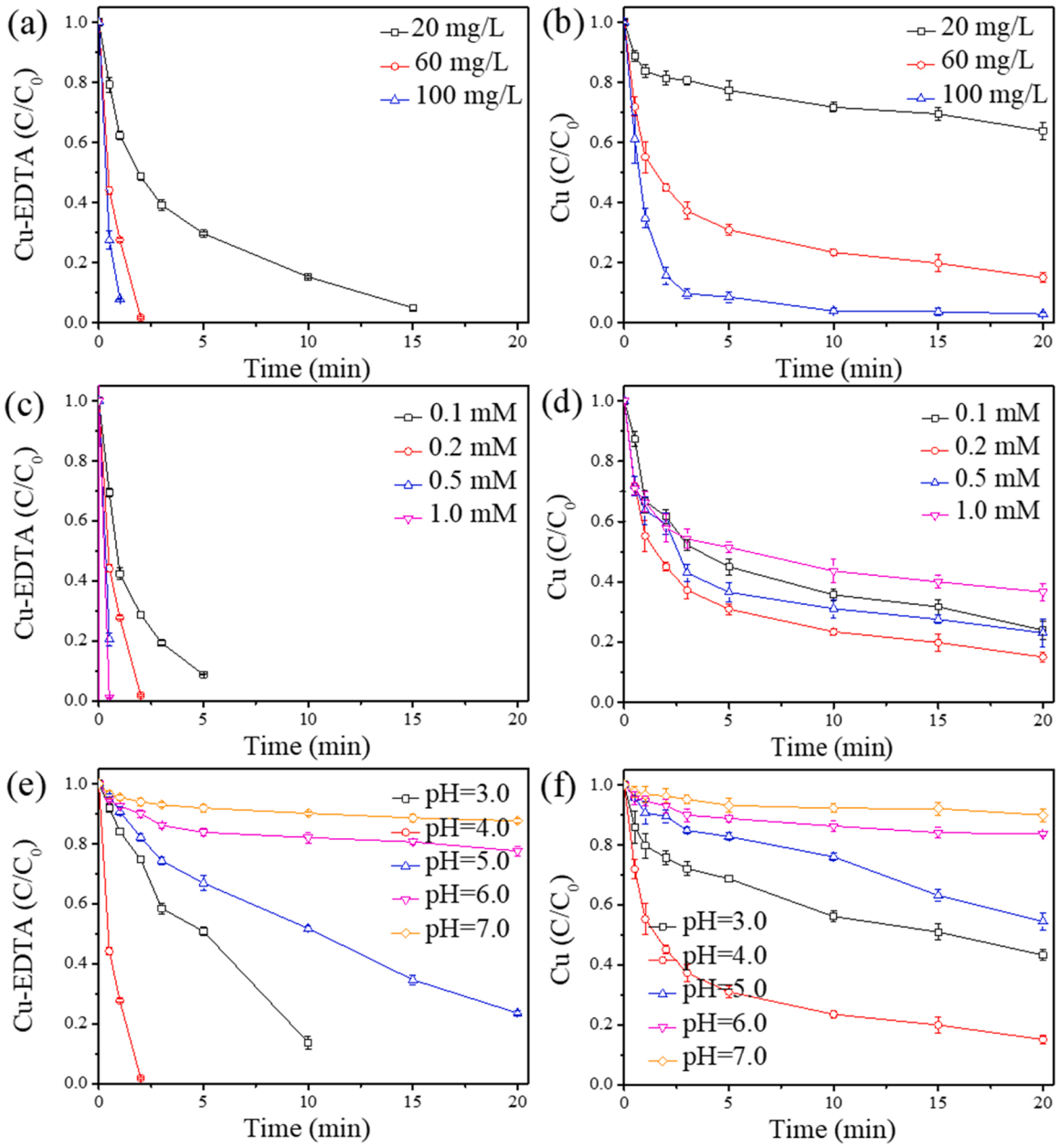

Fig. 7. Effect of (a-b) $Ti_3C_2T_x$, (c-d) PMS concentration and (e-f) solution pH on the decomplexation of Cu-EDTA and the Cu recovery in $Ti_3C_2T_x$/PMS process. All conditions are the same except for the explored variates. Conditions: $[Cu\text{-}EDTA]_0 = 10$ μM, $[PMS]_0 = 0.2$ mM, $[Ti_3C_2T_x]_0 = 60$ mg L^{-1}, $[pH]_0 = 4.0$, and T = 25 °C.

$Ti_3C_2T_x$ was below zero in the investigated pH range (Fig. S9), indicating that $Ti_3C_2T_x$ could effectively adsorb Cu ions. Fig. 7e had verified that Cu-EDTA decomplexation was significantly affected by solution pH. Therefore, influence of solution pH on Cu recovery was mainly related to the decomplexation of Cu-EDTA rather than Cu ions absorption.

3.6. Recycling stability and realistic application

The recycling stability of catalyst is of great important for realistic application. As shown in Fig. 8, complete removal of Cu-EDTA was still achieved within 10 min reaction time after four cycles. However, Cu recovery efficiency dropped sharply, and there was even a slight increase of Cu concentration in the fifth cycle. This was because that longtime reaction led to the oxidation of $Ti_3C_2T_x$, and thus to cause the decrease of adsorption sites and the desorption of Cu ions [15]. To investigate the feasibility of $Ti_3C_2T_x$/PMS process in the treatment of realistic effluent containing Cu-EDTA, Cu recovery and COD removal from electroplating wastewater in $Ti_3C_2T_x$/PMS process were investigated. The basic properties of the electroplating effluent were shown in Table S1. As shown in Fig. 8, the removal efficiency of Cu reached 82.2% and about 30.0% of COD removal was achieved. This satisfactory result further demonstrated the potential application of $Ti_3C_2T_x$/PMS process in the treatment of realistic effluent containing Cu-EDTA.

3.7. Proposed Mechanism

Based on the above discussions, the underlying mechanism of Cu-EDTA decomplexation and Cu recovery in $Ti_3C_2T_x$/PMS process was proposed in Scheme 1. Cu-EDTA decomplexation and Cu recovery were achieved by the following three steps: (I) Initiation. Low-valent Ti exposed on the surface of $Ti_3C_2T_x$ activated PMS and generated few $HO^{\bullet}$ and $SO4^{\bullet-}$. These free radicals attacked Cu-EDTA , which led to the decomplexation of Cu-EDTA and release of Cu ions (Eqs. (1)–(3));

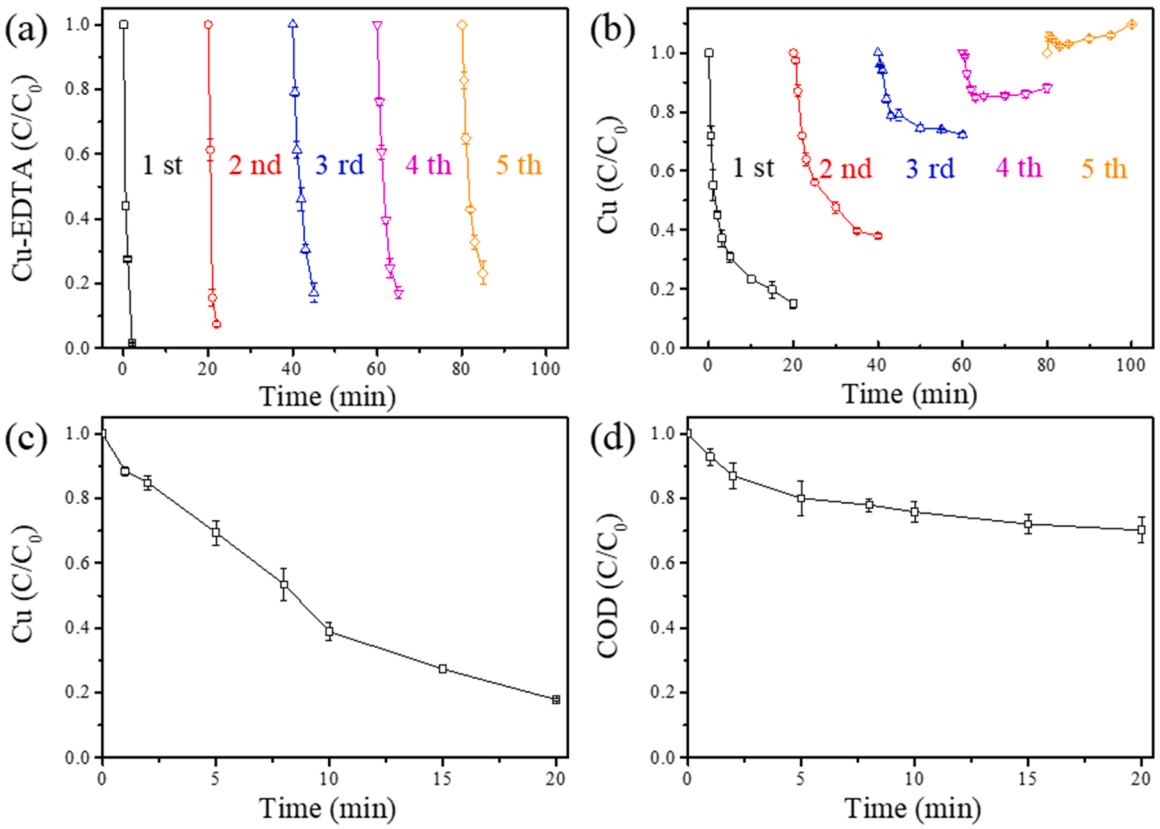

Fig. 8. (a-b) Recycling stability of $Ti_3C_2T_x$ in $Ti_3C_2T_x$/PMS process. Conditions: $[Cu\text{-}EDTA]_0 = 10$ μM, $[PMS]_0 = 0.2$ mM, $[Ti_3C_2T_x]_0 = 60$ mg L^{-1}, $[pH]_0 = 4.0$, and T = 25 °C. (c-d) Cu recovery and COD removal from electroplating wastewater. Conditions: $[Ti_3C_2T_x]_0 = 2.15$ g L^{-1}, $[PMS]_0 = 7.2$ mM.

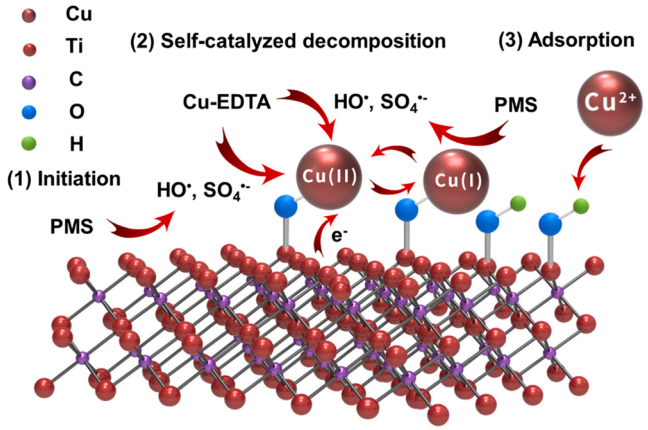

Scheme 1. Schematic diagram of the self-catalyzed decomplexation mechanism of Cu-EDTA in $Ti_3C_2T_x$/PMS process.

$$Ti_3C_2T_X + HSO_5^- \rightarrow SO_4^{\bullet -} + Oxidized Ti_3C_2T_X + OH^- \quad (1)$$

$$Ti_3C_2T_X + HSO_5^- \rightarrow SO_4^{2-} + Oxidized Ti_3C_2T_X + {}^{\bullet}OH \quad (2)$$

$$HO^{\bullet} + SO_4^{\bullet -} + Cu - EDTA \rightarrow Cu^{2+} + Products \quad (3)$$

(II) Self-catalyzed decomplexation of Cu-EDTA. The oxygen-containing functional groups on $Ti_3C_2T_x$ surface bonded with Cu ions and formed the Ti-O-Cu bond (denoted as Ti_3C_2-O-Cu(II), Eq. (4)). Because of the strong reductivity of Ti atoms in $Ti_3C_2T_x$, Cu(II) was reduced to Cu(I) (Eq. (5)). Cu(I) species activated PMS to generate more $HO^{\bullet}$ and $SO4^{\bullet -}$ (Eqs. (6)–(7)), which in turn promoted the decomplexation of Cu-EDTA and released more Cu ions. The construction of Ti-O-Cu bond achieved in situ Cu(II)/Cu(I) cycle and accelerated electron transfer from $Ti_3C_2T_x$ to Cu. Then, the self-catalyzed decomplexation of Cu-EDTA was achieved by utilizing the trace Cu(II) inherent in Cu-EDTA without addition of extraneous transition metals;

$$Ti_3C_2T_x + Cu^{2+} \rightarrow Ti_3C_2 - O - Cu(II) \quad (4)$$

$$Ti_3C_2 - O - Cu(II) \rightarrow Ti_3C_2 - O - Cu(I) \quad (5)$$

$$Ti_3C_2 - O - Cu(I) + HSO_5^- \rightarrow Ti_3C_2 - O - Cu(II) + OH^- + SO_4^{\bullet -} \quad (6)$$

$$Ti_3C_2 - O - Cu(I) + HSO_5^- \rightarrow Ti_3C_2 - O - Cu(II) + {}^{\bullet}OH + SO_4^{2-} \quad (7)$$

(III) Cu recovery. The decomposition products of Cu-EDTA could also achieve self-catalyzed decomplexation in $Ti_3C_2T_x$/PMS process (Fig. 3b). After decomplexation reaction, Cu ions were released and absorbed on the negative charged surface of $Ti_3C_2T_x$.

4. Conclusions

The combination of $Ti_3C_2T_x$ and PMS achieved efficient decomplexation of Cu-EDTA complex and recovery of Cu without addition of extraneous transition metals. The trace Cu(II) inherent in Cu-EDTA was utilized to active PMS and achieve the self-catalyzed decomplexation of Cu-EDTA. A novel self-catalyzed decomplexation mechanism of Cu-EDTA including initiation reaction, self-catalyzed decomplexation and Cu recovery was proposed. $Ti_3C_2T_x$ played the triple roles as initiation reagent for radicals generation, reductant for triggering Cu(II)/Cu(I) cycle and absorbent for Cu ions recovery. Compared with hydroxylamine and ascorbic acid, $Ti_3C_2T_x$ exhibited superior performance for PMS activation. In addition, about 82.2% Cu and 30.0% COD were removed within 20 min from realistic electroplating effluent in $Ti_3C_2T_x$/PMS process. This study provided a feasible way to remove heavy metal

complexes and recovery of heavy metals from wastewater.

CRediT authorship contribution statement

Daoyuan Zu: Methodology, Investigation, Data curation, Formal analysis and Writing – original draft. **Haoran Song:** Data curation, Formal analysis, Writing – review & editing. **Changping Li:** Methodology, Investigation, Writing – review & editing, Supervision. **Yuwei Wang:** Methodology. **Rong Du:** Data curation. **Rui Zhou**: Formal analysis. **Wei Zhang:** Methodology. **Shiting Pan:** Methodology. **Yang Cai**: Formal analysis. **Yongming Shen:** Writing – review & editing. **Zhifeng Yang:** Writing – review & editing, Supervision, Project administration, Resources.

Declaration of Competing Interest

The authors declare that they have no known competing financial interests or personal relationships that could have appeared to influence the work reported in this paper.

Acknowledgements

This study was funded by the Key Special Project for Introduced Talents Team of Southern Marine Science and Engineering Guangdong Laboratory (Guangzhou) under Grant No. GML2019ZD0403, the Program for Guangdong Introducing Innovative and Entrepreneurial Teams under Grant No. 2019ZT08L213 and Guangdong Provincial Key Laboratory Project Grant No. 2019B121203011.

Appendix A. Supporting information

Supplementary data associated with this article can be found in the online version at doi:10.1016/j.apcatb.2022.121131.

References

[1] Y.L. Lu, S. Song, R.S. Wang, Z.Y. Liu, J. Meng, A.J. Sweetman, A. Jenkins, R. C. Ferrier, H. Li, W. Luo, T.Y. Wang, Impacts of soil and water pollution on food safety and health risks in China, Environ. Int. 77 (2015) 5–15, https://doi.org/10.1016/j.envint.2014.12.010.

[2] S.S. Ye, Y.X. Chen, X.L. Yao, J.D. Zhang, Simultaneous removal of organic pollutants and heavy metals in wastewater by photoelectrocatalysis: a review, Chemosphere 273 (2021) 12, https://doi.org/10.1016/j.chemosphere.2020.128503.

[3] Y. Zhang, X.Y. Cai, X.M. Lang, X.L. Qiao, X.H. Li, J.W. Chen, Insights into aquatic toxicities of the antibiotics oxytetracycline and ciprofloxacin in the presence of metal: complexation versus mixture, Environ. Pollut. 166 (2012) 48–56, https://doi.org/10.1016/j.envpol.2012.03.009.

[4] A. Crémazy, K.V. Brix, C.M. Wood, Chronic toxicity of binary mixtures of six metals (Ag, Cd, Cu, Ni, Pb, and Zn) to the great pond snail Lymnaea stagnalis, Environ. Sci. Technol. 52 (2018) 5979–5988, https://doi.org/10.1021/acs.est.7b06554.

[5] Z. Xu, G.D. Gao, B.C. Pan, W.M. Zhang, L. Lv, A new combined process for efficient removal of Cu(II) organic complexes from wastewater: Fe(III) displacement/UV degradation/alkaline precipitation, Water Res. 87 (2015) 378–384, https://doi.org/10.1016/j.watres.2015.09.025.

[6] M. Pan, C. Zhang, J. Wang, J.W. Chew, G. Gao, B. Pan, Multifunctional piezoelectric heterostructure of $BaTiO_3$@ Graphene: decomplexation of Cu-EDTA and recovery of Cu, Environ. Sci. Technol. 53 (2019) 8342–8351, https://doi.org/10.1021/acs.est.9b02355.

[7] Y. Cao, X.C. Qian, Y.X. Zhang, G.Z. Qu, T.J. Xia, X.T. Guo, H.Z. Jia, T.C. Wang, Decomplexation of EDTA-chelated copper and removal of copper ions by non-thermal plasma oxidation/alkaline precipitation, Chem. Eng. J. 362 (2019) 487–496, https://doi.org/10.1016/j.cej.2019.01.061.

[8] Y.X. Ye, C. Shan, X.L. Zhang, H. Liu, D.D. Wang, L. Lv, B.C. Pan, Water decontamination from Cr(III)-organic complexes based on pyrite/H_2O_2: performance, mechanism, and validation, Environ. Sci. Technol. 52 (2018) 10657–10664, https://doi.org/10.1021/acs.est.8b01693.

[9] H.B. Zeng, S.S. Liu, B.Y. Chai, D. Cao, Y. Wang, X. Zhao, Enhanced photoelectrocatalytic decomplexation of Cu-EDTA and Cu recovery by persulfate activated by UV and cathodic reduction, Environ. Sci. Technol. 50 (2016) 6459–6466, https://doi.org/10.1021/acs.est.6b00632.

[10] Z. Xu, C. Shan, B.H. Xie, Y. Liu, B.C. Pan, Decomplexation of Cu(II)-EDTA by UV/persulfate and UV/H_2O_2: efficiency and mechanism, Appl. Catal. B Environ. 200 (2017) 439–447, https://doi.org/10.1016/j.apcatb.2016.07.023.

[11] S.S. Lee, H.W. Bai, Z.Y. Liu, D.D. Sun, Green approach for photocatalytic Cu(II)-EDTA degradation over TiO_2: toward environmental sustainability, Environ. Sci. Technol. 49 (2015) 2541–2548, https://doi.org/10.1021/es504711e.

[12] X. Huang, Y. Xu, C. Shan, X. Li, W. Zhang, B. Pan, Coupled Cu(II)-EDTA degradation and Cu(II) removal from acidic wastewater by ozonation: performance, products and pathways, Chem. Eng. J. 299 (2016) 23–29, https://doi.org/10.1016/j.cej.2016.04.044.

[13] A.D. Bokare, W. Choi, Review of iron-free Fenton-like systems for activating H_2O_2 in advanced oxidation processes, J. Hazard. Mater. 275 (2014) 121–135, https://doi.org/10.1016/j.jhazmat.2014.04.054.

[14] H. Song, D. Zu, C. Li, R. Zhou, Y. Wang, W. Zhang, S. Pan, Y. Cai, Z. Li, Y. Shen, Ultrafast activation of peroxymonosulfate by reduction of trace Fe^{3+} with Ti_3C_2 MXene under neutral and alkaline conditions: reducibility and confinement effect, Chem. Eng. J. 423 (2021), 130012, https://doi.org/10.1016/j.cej.2021.130012.

[15] A. Shahzad, K. Rasool, W. Miran, M. Nawaz, J. Jang, K.A. Mahmoud, D.S. Lee, Two-dimensional $Ti_3C_2T_x$ MXene nanosheets for efficient copper removal from water, ACS Sustain. Chem. Eng. 5 (2017) 11481–11488, https://doi.org/10.1021/acssuschemeng.7b02695.

[16] Y.L. Ying, Y. Liu, X.Y. Wang, Y.Y. Mao, W. Cao, P. Hu, X.S. Peng, Two-dimensional titanium carbide for efficiently reductive removal of highly toxic chromium(VI) from water, ACS Appl. Mater. Interfaces 7 (2015) 1795–1803, https://doi.org/10.1021/am5074722.

[17] R.P. Pandey, K. Rasool, V.E. Madhavan, B. Aissa, Y. Gogotsi, K.A. Mahmoud, Ultrahigh-flux and fouling-resistant membranes based on layered silver/MXene ($Ti_3C_2T_x$) nanosheets, J. Mater. Chem. A 6 (2018) 3522–3533, https://doi.org/10.1039/c7ta10888e.

[18] L. Wang, H. Song, L.Y. Yuan, Z.J. Li, Y.J. Zhang, J.K. Gibson, L.R. Zheng, Z.F. Chai, W.Q. Shi, Efficient U(VI) reduction and sequestration by Ti_2CT_x MXene, Environ. Sci. Technol. 52 (2018) 10748–10756, https://doi.org/10.1021/acs.est.8b03711.

[19] L. Wang, H. Song, L.Y. Yuan, Z.J. Li, P. Zhang, J.K. Gibson, L.R. Zheng, H.Q. Wang, Z.F. Chai, W.Q. Shi, Effective removal of anionic Re(VII) by surface-modified Ti_2CT_x MXene nanocomposites: implications for Tc(VII) sequestration, Environ. Sci. Technol. 53 (2019) 3739–3747, https://doi.org/10.1021/acs.est.8b07083.

[20] Q.M. Peng, J.X. Guo, Q.R. Zhang, J.Y. Xiang, B.Z. Liu, A.G. Zhou, R.P. Liu, Y. J. Tian, Unique lead adsorption behavior of activated hydroxyl group in two-dimensional titanium carbide, J. Am. Chem. Soc. 136 (2014) 4113–4116, https://doi.org/10.1021/ja500506k.

[21] A. Shahzad, K. Rasool, W. Miran, M. Nawaz, J. Jang, K.A. Mahmoud, D.S. Lee, Mercuric ion capturing by recoverable titanium carbide magnetic nanocomposite, J. Hazard. Mater. 344 (2018) 811–818, https://doi.org/10.1016/j.jhazmat.2017.11.026.

[22] M. Alhabeb, K. Maleski, B. Anasori, P. Lelyukh, L. Clark, S. Sin, Y. Gogotsi, Guidelines for synthesis and processing of two-dimensional titanium carbide ($Ti_3C_2T_x$ MXene), Chem. Mater. 29 (2017) 7633–7644, https://doi.org/10.1021/acs.chemmater.7b02847.

[23] C.J. Liang, C.F. Huang, N. Mohanty, R.M. Kurakalva, A rapid spectrophotometric determination of persulfate anion in ISCO, Chemosphere 73 (2008) 1540–1543, https://doi.org/10.1016/j.chemosphere.2008.08.043.

[24] J.L. Wang, S.Z. Wang, Activation of persulfate (PS) and peroxymonosulfate (PMS) and application for the degradation of emerging contaminants, Chem. Eng. J. 334 (2018) 1502–1517, https://doi.org/10.1016/j.cej.2017.11.059.

[25] A. Rastogi, S.R. Ai-Abed, D.D. Dionysiou, Sulfate radical-based ferrous-peroxymonosulfate oxidative system for PCBs degradation in aqueous and sediment systems, Appl. Catal. B Environ. 85 (2009) 171–179, https://doi.org/10.1016/j.apcatb.2008.07.010.

[26] Y.M. Ren, L.Q. Lin, J. Ma, J. Yang, J. Feng, Z.J. Fan, Sulfate radicals induced from peroxymonosulfate by magnetic ferrospinel MFe_2O_4 (M= Co, Cu, Mn, and Zn) as heterogeneous catalysts in the water, Appl. Catal. B Environ. 165 (2015) 572–578, https://doi.org/10.1016/j.apcatb.2014.10.051.

[27] Q. Ye, H. Xu, J. Zhang, Q.G. Wang, P. Zhou, Y.Q. Wang, X. Huang, X.W. Huo, C. R. Liu, J.F. Lu, Enhancement of peroxymonosulfate activation for antibiotics removal by nano zero valent tungsten induced Cu(II)/Cu(I) redox cycles, Chem. Eng. J. 382 (2020) 12, https://doi.org/10.1016/j.cej.2019.123054.

[28] Y. Yao, Y. Cai, G. Wu, F. Wei, X. Li, H. Chen, S. Wang, Sulfate radicals induced from peroxymonosulfate by cobalt manganese oxides ($Co_xMn_{3-x}O_4$) for Fenton-Like reaction in water, J. Hazard. Mater. 296 (2015) 128–137, https://doi.org/10.1016/j.jhazmat.2015.04.014.

[29] Y. Yao, H. Chen, C. Lian, F. Wei, D. Zhang, G. Wu, B. Chen, S. Wang, Fe, Co, Ni nanocrystals encapsulated in nitrogen-doped carbon nanotubes as Fenton-like catalysts for organic pollutant removal, J. Hazard. Mater. 314 (2016) 129–139.

[30] M.M. Ding, W. Chen, H. Xu, C.H. Lu, T. Lin, Z. Shen, H. Tao, K. Zhang, Synergistic features of superoxide molecule anchoring and charge transfer on two-dimensional $Ti_3C_2T_x$ MXene for efficient peroxymonosulfate activation, ACS Appl. Mater. Interfaces 12 (2020) 9209–9218, https://doi.org/10.1021/acsami.9b20530.

[31] J.Y. Li, J.X. Ma, R.B. Dai, X.Y. Wang, M. Chen, T.D. Waite, Z.W. Wang, Self-enhanced decomplexation of Cu-organic complexes and Cu recovery from wastewaters using an electrochemical membrane filtration system, Environ. Sci. Technol. 55 (2021) 655–664, https://doi.org/10.1021/acs.est.0c05554.

[32] P. Nfodzo, H. Choi, Triclosan decomposition by sulfate radicals: effects of oxidant and metal doses, Chem. Eng. J. 174 (2011) 629–634, https://doi.org/10.1016/j.cej.2011.09.076.

[33] Y.B. Ding, H.B. Tang, S.H. Zhang, S.B. Wang, H.Q. Tang, Efficient degradation of carbamazepine by easily recyclable microscaled $CuFeO_2$ mediated heterogeneous activation of peroxymonosulfate, J. Hazard. Mater. 317 (2016) 686–694, https://doi.org/10.1016/j.jhazmat.2016.06.004.

[34] J.F. Yan, J. Li, J.L. Peng, H. Zhang, Y.H. Zhang, B. Lai, Efficient degradation of sulfamethoxazole by the $CuO@Al_2O_3$ (EPC) coupled PMS system: optimization, degradation pathways and toxicity evaluation, Chem. Eng. J. 359 (2019) 1097–1110, https://doi.org/10.1016/j.cej.2018.11.074.

[35] J. Halim, K.M. Cook, M. Naguib, P. Eklund, Y. Gogotsi, J. Rosen, M.W. Barsoum, X-ray photoelectron spectroscopy of select multi-layered transition metal carbides (MXenes), Appl. Surf. Sci. 362 (2016) 406–417, https://doi.org/10.1016/j.apsusc.2015.11.089.

[36] Y.H. Xu, D.H. Liang, M.L. Liu, D.Z. Liu, Preparation and characterization of Cu_2O-TiO_2: efficient photocatalytic degradation of methylene blue, Mater. Res. Bull. 43 (2008) 3474–3482, https://doi.org/10.1016/j.materresbull.2008.01.026.

[37] X.B. Wang, N. Chen, X.F. Liu, Y.B. Shi, C.C. Ling, L.Z. Zhang, Ascorbate guided conversion of hydrogen peroxide to hydroxyl radical on goethite, Appl. Catal. B Environ. 282 (2021) 7, https://doi.org/10.1016/j.apcatb.2020.119558.

[38] H.Z. Chi, X. He, J.Q. Zhang, D. Wang, X.D. Zhai, J. Ma, Hydroxylamine enhanced degradation of naproxen in Cu^{2+} activated peroxymonosulfate system at acidic condition: efficiency, mechanisms and pathway, Chem. Eng. J. 361 (2019) 764–772, https://doi.org/10.1016/j.cej.2018.12.114.

[39] Y.H. Guan, J. Ma, X.C. Li, J.Y. Fang, L.W. Chen, Influence of pH on the formation of sulfate and hydroxyl radicals in the UV/peroxymonosulfate system, Environ. Sci. Technol. 45 (2011) 9308–9314, https://doi.org/10.1021/Es2017363.

[40] T. Zhang, H.B. Zhu, J.P. Croue, Production of sulfate radical from peroxymonosulfate induced by a magnetically separable $CuFe_2O_4$ spinel in water: efficiency, stability, and mechanism, Environ. Sci. Technol. 47 (2013) 2784–2791, https://doi.org/10.1021/Es304721g.